

# Influence of self-disassembly of bridges on collective flow characteristics of swarm robots in a single-lane and periodic system with a gap

Kotaro Ito<sup>a</sup>, Ryosuke Nishi<sup>b,\*</sup>

<sup>a</sup>Department of Engineering, Graduate School of Sustainability Science, Tottori University, 4-101 Koyama-cho Minami, Tottori 680-8552, Japan.

<sup>b</sup>Department of Mechanical and Physical Engineering, Faculty of Engineering, Tottori University, 4-101 Koyama-cho Minami, Tottori 680-8552, Japan.

---

## Abstract

Inspired by the living bridges formed by ants, swarm robots have been developed to self-assemble bridges to span gaps and self-disassemble them. Self-disassembly of bridges may increase the transport efficiency of swarm robots by increasing the number of moving robots, and also may decrease the efficiency by causing gaps to reappear. Our aim is to elucidate the influence of self-disassembly of bridges on the collective flow characteristics of swarm robots in a single-lane and periodic system with a gap. In the system, robots span and cross the gap by self-assembling a single-layer bridge. We consider two scenarios in which self-disassembling bridges is prevented (prevent-scenario) or allowed (allow-scenario). We represent the horizontal movement of robots with a typical car-following model, and simply model the actions of robots for self-assembling and self-disassembling bridges. Numerical simulations have revealed the following results. Flow-density diagrams in both the scenarios shift to the higher-density region as the gap length increases. When density is low, allow-scenario exhibits the steady state of repeated self-assembly and self-disassembly of bridges. If density is extremely low, flow in this state is greater than flow in prevent-scenario owing to the increase in the number of robots moving horizontally. Otherwise, flow in this state is smaller than flow in prevent-scenario. Besides, flow in this state increases monotonically with respect to the velocity of robots in joining and leaving bridges. Thus, self-disassembling bridges is recommended for only extremely low-density conditions in periodic systems. This study contributes to the development of the collective dynamics of self-driven particles that self-assemble structures, and stirs the dynamics with other self-assembled structures, such as ramps, chains, and towers.

**Keywords:** Swarm robot, Collective dynamics, Self-assembly, Self-disassembly, Bridge, Periodic system

---

## 1. Introduction

Swarm robotics treats a large number of robots that locally interact with other robots and the environment, and aims to achieve robust, scalable, and flexible collective behaviors of robots emerging from the interactions [1]. Swarm robots realize various collective behaviors that are categorized into four types: spatially organizing behaviors (e.g., self-assembly), navigation behaviors (e.g., collective exploration), collective decision-making (e.g., consensus achievement), and other collective behaviors (e.g., collective fault detection) [2].

When robots explore an unfamiliar field, they may be faced with obstacles they can not go through, such as steps and gaps. Robots overcome the obstacles by the following ways. In the first way, robots pass over the obstacles without modifying the environment by physically jointing with each other [3–7] or mutually transporting each other [8]. The second and third ways modify the environment. In the second way, robots construct structures using external materials other than themselves [9–11]. In the third way, robots construct structures using their own bodies, that is, robots self-assemble structures to overcome the obstacles, such as ramps to pass over a step [12], and bridges to span a gap (e.g., bridges self-assembled from both directions [13]). In this study, we focus on self-assembled swarm-robot bridges to

---

\*Corresponding author. Tel.: +81 857 31 5192; fax: +81 857 31 5210.

Email address: nishi@tottori-u.ac.jp (Ryosuke Nishi)

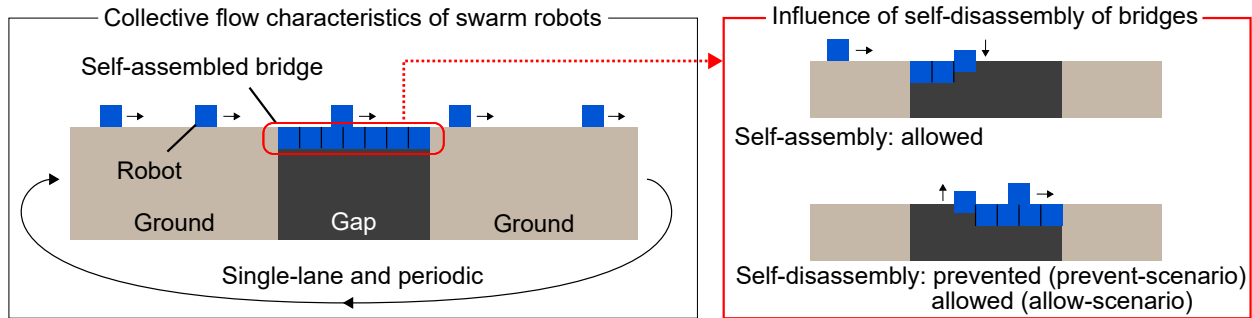


Figure 1: Schematic diagram of this study. This study numerically investigates the influence of self-disassembly of bridges on the collective flow characteristics of swarm robots on a single-lane and periodic system with a gap. We use two scenarios: prevent-scenario and allow-scenario. Both the scenarios allow the self-assembly of bridges. Prevent-scenario prevents the self-disassembly of bridges, and allow-scenario allows it.

span a gap, which are generally inspired by living ant bridges self-assembled by ants (more specifically, weaver and army ants) [14–16].

We review the related work on self-assembly of bridges to span a gap formed by robots and ants. In swarm robotics and the neighboring modular robotics, Pamecha et al. [17] illustrated a concept of self-assembled bridge-like robot structures as a possible application of modular robots, and Hosokawa et al. [18] illustrated a concept of self-assembled robot bridges to cross a gap. Walter et al. [19] investigated the self-reconfiguration of hexagonal robots from chains to bridge-like structures by numerical simulations. Inou et al. [20] investigated the influence of mechanical properties on self-assembled bridge-like robot structures to convey a moving load. Moreover, Inou et al. [21] examined the information processing functions of robots required for a mission to self-assemble and self-disassemble the structures, and developed an algorithm for the mission. Furthermore, motion mechanisms for the structures were proposed [22, 23]. Later, Suzuki et al. [24] proposed an algorithm for robots to self-assemble bridge-like structures adaptively in response to load conditions. Bray and Groß [25] developed sequential and parallel algorithms for robots to self-assemble cantilevers. Besides, Bray and Groß [26] developed algorithms for robots to optimally reduce the number of robots belonging to the self-assembled bridges, and to dismantle them. Nguyen-Duc et al. [27] reported the self-assembly and self-disassembly of robot bridges based on a distributed control using numerical simulations. Malley et al. [28] developed a soft-robot system named *Eciton robotica*, and numerically demonstrated that the robots self-assembled and self-disassembled a bridge in response to the local traffic density and the V-shaped gap angle. Swisler and Rubenstein [13] developed an algorithm for swarm robots to self-assemble amorphous and environment-adaptive three-dimensional structures including cantilevers, and bridges formed from both directions. Andrés Arroyo et al. [29] proposed a stochastic algorithm for programmable matter to self-assemble shortcut bridges. Sugawara et al. [30] investigated a casualty-based cooperation of swarm robots such that robots overcame a ditch by moving on the dead robots that had unintentionally fallen into the ditch. Self-assembled floating-robot structures including floating bridges were also proposed [31, 32]. In the research field of the collective behavior of ants, self-assembled living ant bridges were investigated in terms of the robustness and reactivity of bridges [33], and the dynamical adjustment and optimization of them [34]. Two-dimensional multi-agent systems were developed for reproducing the self-assembly of living ant bridges [35], and investigating the foraging behavior of ants under the presence of self-assembled living ant bridges to span a gap [36, 37].

It is well known that the systems in which agents (including robots and ants) self-assemble bridges to span a gap contain trade-offs between the benefit brought by the bridges and the cost caused by them. For instance, Reid et al. [34] demonstrated that army ants dynamically adjusted the positions of the self-assembled living ant bridges to balance the benefit of the increase in the foraging efficiency brought by the bridges against the cost of the decrease in moving ants due to the formation of the bridges. Andrés Arroyo et al. [29] produced self-assembled programmable-matter bridges by numerical simulations, and the bridges balanced the benefit of the shortened path length against the cost of the bridges. In this paper, we consider another cost-benefit trade-off in the swarm robot systems with self-assembled bridges to span a gap: the trade-off in terms of the transport efficiency of swarm robots under the presence of the self-disassembly of bridges. Self-disassembly of a bridge increases the number of exploring robots, which may increase the transport efficiency of robots. On the other hand, self-disassembly of a bridge causes the gap

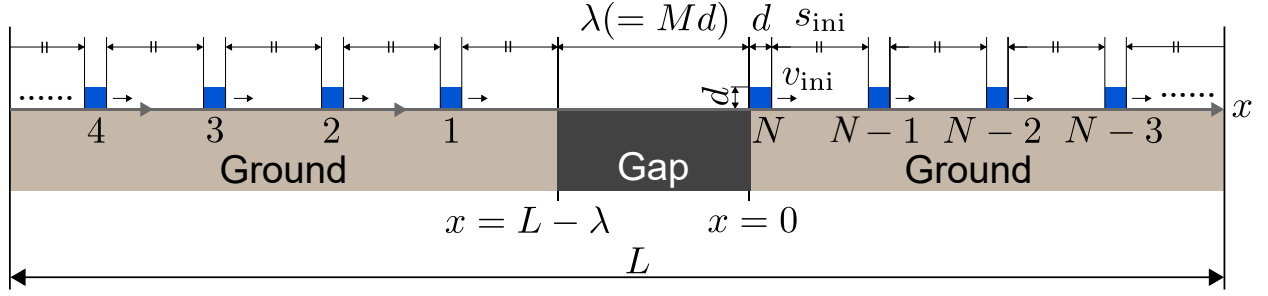


Figure 2: Initial conditions of the periodic system with a gap. The system length is  $L$ . The gap length is  $\lambda (= Md)$ . The length and height of each robot are  $d$ . Positions of the left (upstream) and right (downstream) edges of the gap is  $x = L - \lambda$  and  $x = 0$ , respectively. The front edge of robot 1 is initially placed upstream of the left edge of the gap by  $s_{\text{ini}}$ . Robots  $2, \dots, N$  have the same initial forward spacing  $s_{\text{ini}}$ . The rear edge of robot  $N$  is initially placed at the right edge of the gap. All robots have the same initial velocity  $v_{\text{ini}}$ , which is the equilibrium velocity of IDM at the forward spacing  $s_{\text{ini}}$ .

to reappear, and disrupts the movement of robots to cross the gap till robots reconstruct the next bridge. Therefore, self-disassembly of bridges may have significant influence on the collective flow characteristics of swarm robots (such as the flow-density relationship), and we need to clarify the sole effect of the self-disassembly. As a first step, it is reasonable to simplify the system as much as possible, that is, use a one-dimensional system (such as a single-lane and periodic system with a gap) rather than two or higher dimensional systems [13, 28, 29, 35–37]. Therefore, our aim is to elucidate the influence of self-disassembly of bridges on the collective flow characteristics of swarm robots in a single-lane and periodic system with a gap as shown in Fig. 1. In the system, swarm robots move in one direction on a single-lane road, and pass over the gap by self-assembling a bridge. To this aim, we consider two scenarios. The first scenario (named prevent-scenario) prevents robots from self-disassembling bridges. In this scenario, robots self-assemble a bridge only once, and the bridge permanently remains. The second scenario (named allow-scenario) allows robots to self-disassemble bridges, and self-assemble new bridges. We represent the horizontal movement of robots using intelligent driver model (IDM) [38, 39] as a typical car-following model, and simply model the actions of robots for the self-assembly and self-disassembly of bridges. We investigate the relation between flow and density of swarm robots for the two scenarios and various gap lengths using numerical simulations.

Since swarm robot is a kind of self-driven particle (SDP), which includes vehicle, pedestrian, insect, and molecular motor, this study contributes to further understanding and development of the collective dynamics of SDPs [40–42].

The rest of this paper is organized as follows. We model the system in Sec. 2. We show the results in Sec. 3, and present the conclusive discussion in Sec. 4.

## 2. Model

We consider a periodic system which has a single-lane road with a gap (such as a deep valley) as shown in Fig. 2. The system length is  $L$  (m), and the gap length is  $\lambda$  (m). We assume that  $\lambda$  is a non-negative integer multiple of the length of each robot  $d = 0.1$  m, that is,  $\lambda = Md$  ( $M = 0, 1, 2, \dots$ ). When  $\lambda = 0$  m (that is,  $M = 0$ ), no gap exists in the system. Position  $x$  (m) is zero at the right (downstream) edge of the gap, increases in the right direction, is  $L - \lambda$  at the left (upstream) edge of the gap, and returns to zero at the right edge of the gap. Hence the range of  $x$  is given by  $[0, L)$ . The system has  $N$  robots named robots  $1, 2, \dots, N$ . The height of each robot is equal to its length  $d$ . We define  $x_i(t)$  (m) as the position of the front edge of robot  $i$  at time  $t$  (s), and  $v_i(t)$  (m/s) as its velocity at time  $t$ . All robots move to the right (that is, in the positive  $x$  direction). We define density as  $\rho = N/L$  (robots/m). In the middle of each run of numerical simulations, no new robot appears in the system, and no robot leaves the system. Hence  $N$  and  $\rho$  are constant throughout each run.

### 2.1. Initial conditions

At the initial time  $t = 0$  s, all robots are placed on the continuous section of length  $L - \lambda$  as shown in Fig. 2. Robot  $N$ 's rear edge is initially placed at the right edge of the gap ( $x = 0$  m). Robot  $N$  has the initial forward spacing  $s_{\text{ini}}$  (m). Robot  $N - 1$  is initially placed just downstream (ahead) of robot  $N$ ; hence, the rear edge of robot  $N - 1$  is initially

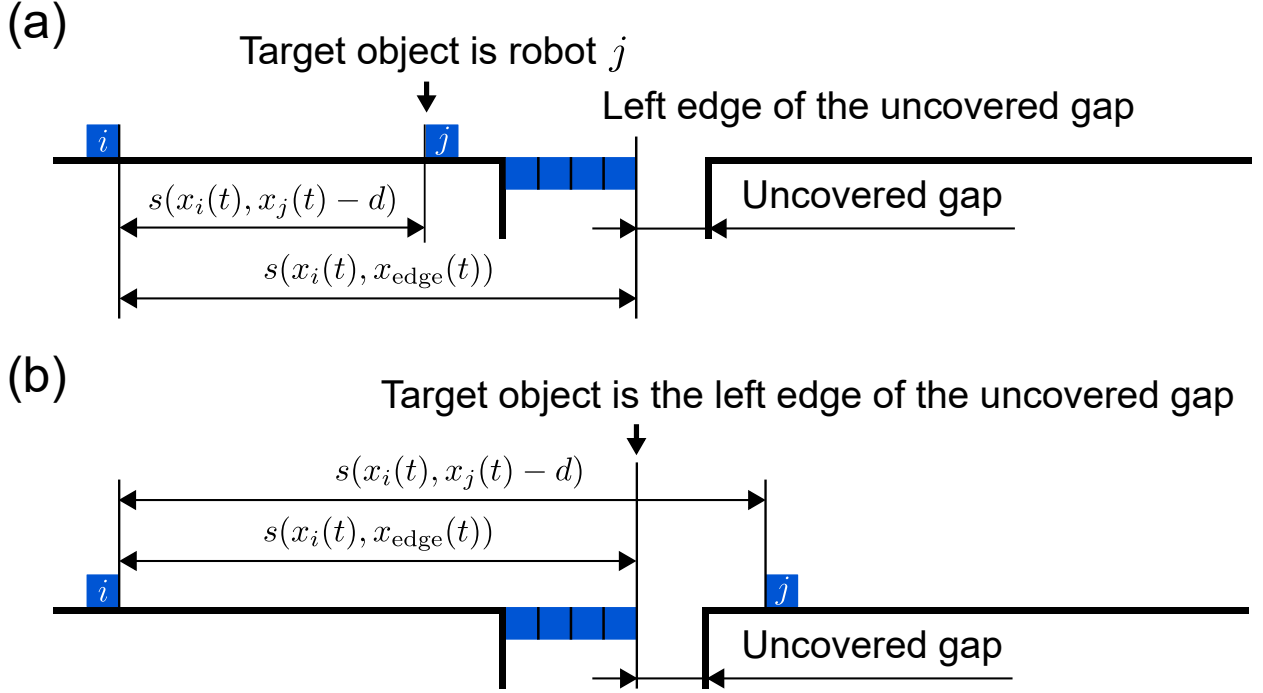


Figure 3: The target object of robot  $i$ . (a) Forward spacing  $s(x_i(t), x_j(t) - d)$  is smaller than or equal to  $s(x_i(t), x_{\text{edge}}(t))$ . The target object of robot  $i$  is robot  $j$ . (b) Forward spacing  $s(x_i(t), x_j(t) - d)$  is greater than  $s(x_i(t), x_{\text{edge}}(t))$ . The target object of robot  $i$  is the left (upstream) edge of the uncovered gap.

placed at  $x = d + s_{\text{ini}}$ . Besides, robot  $N - 1$  has the same initial forward spacing  $s_{\text{ini}}$  as robot  $N$ . In the same way, robot  $i$ 's rear edge is initially placed at  $x = (N - i)(d + s_{\text{ini}})$  for  $i = 1, 2, \dots, N$ , and robots  $2, 3, \dots, N$  have the same initial forward spacing  $s_{\text{ini}}$ . Additionally, robot 1's front edge is initially upstream of the left edge of the gap by  $s_{\text{ini}}$ . That is, the initial position of the front edge of robot  $i$  ( $i = 1, \dots, N$ ) is given by

$$x_i(0) = d + (N - i)(d + s_{\text{ini}}), \quad (1)$$

and  $s_{\text{ini}}$  is given by

$$s_{\text{ini}} = \frac{L - \lambda}{N} - d. \quad (2)$$

All robots have the same initial velocity  $v_{\text{ini}}$  (m/s), which is the equilibrium velocity of IDM at the forward spacing  $s_{\text{ini}}$ . We obtain  $v_{\text{ini}}$  by numerically solving the following equation:

$$s_{\text{ini}} = \frac{s_0 + T v_{\text{ini}}}{\sqrt{1 - \left(\frac{v_{\text{ini}}}{v_0}\right)^\delta}}. \quad (3)$$

The definition of IDM is described later in Eq. (9), and Eq. (3) is obtained by setting  $v_i(t) = v_{\text{ini}}$ ,  $s_{\text{eff}}(t) = s_{\text{ini}}$ ,  $dv_i(t)/dt = 0$ , and  $\Delta v_{\text{eff}}(t) = 0$  in Eq. (9). The parameters of IDM appearing in Eq. (3) (that is,  $s_0$ ,  $v_0$ ,  $T$ , and  $\delta$ ) are explained below Eq. (10).

## 2.2. Actions of robots

Each robot has the following functions. (i) It accelerates and decelerates in the forward direction. (ii) It detects the forward edge of the road. (iii) It detects the contact with the ground, walls, and other robots. (iv) It attaches itself

Table 1: Parameter settings of IDM.

$a$	$b$	$s_0$	$v_0$	$T$	$\delta$
0.01 m/s <sup>2</sup>	0.015 m/s <sup>2</sup>	0.02 m	0.1 m/s	1 s	4

to other robots and walls, and detaches itself from them. (v) It ascends and descends. (vi) It communicates with the robots physically connected to itself. (vii) It obtains its own velocity, the spacing and the relative velocity between it and the object in front of it, and the spacing and the relative velocity between it and the object behind it. Each robot can perform the three actions using these functions: following the target object, self-assembling a bridge, and self-disassembling it.

### 2.2.1. Following the target object

We define

$$s(x_1, x_2) = \begin{cases} x_2 - x_1 & \text{if } x_2 \geq x_1, \\ x_2 - x_1 + L & \text{if } x_2 < x_1, \end{cases} \quad (4a)$$

$$(4b)$$

as the forward spacing from position  $x_1$  to position  $x_2$ . Robot  $i$  moves horizontally to the right by following the target object as shown in Figs. 3(a) and (b). A candidate of the target object of robot  $i$  is its preceding robot that is not a complete component of a bridge. This preceding robot is named robot  $j$ . Another candidate is the left edge of the uncovered gap. The uncovered gap is the part of the gap not covered by the complete bridge components. As shown in Fig. 3(a), robot  $i$  selects robot  $j$  as the target object if

$$s(x_i(t), x_j(t) - d) \leq s(x_i(t), x_{\text{edge}}(t)), \quad (5)$$

where position  $x_{\text{edge}}(t)$  is the position of the left edge of the uncovered gap at time  $t$ . As shown in Fig. 3(b), robot  $i$  selects the left edge of the uncovered gap as the target object if

$$s(x_i(t), x_j(t) - d) > s(x_i(t), x_{\text{edge}}(t)). \quad (6)$$

We define  $s_{\text{eff}}(t)$  as the forward spacing from robot  $i$  to the target object at time  $t$ :

$$s_{\text{eff}}(t) = \begin{cases} s(x_i(t), x_j(t) - d) & \text{if the target object is robot } j, \\ s(x_i(t), x_{\text{edge}}(t)) & \text{if the target object is the left edge of the uncovered gap.} \end{cases} \quad (7a)$$

$$(7b)$$

Besides, we define  $\Delta v_{\text{eff}}(t)$  as the relative velocity between robot  $i$  and the target object at time  $t$ :

$$\Delta v_{\text{eff}}(t) = \begin{cases} v_i(t) - v_j(t) & \text{if the target object is robot } j, \\ v_i(t) - 0 = v_i(t) & \text{if the target object is the left edge of the uncovered gap.} \end{cases} \quad (8a)$$

$$(8b)$$

The acceleration of robot  $i$  at time  $t$  is determined by IDM [38, 39] that uses  $s_{\text{eff}}(t)$  and  $\Delta v_{\text{eff}}(t)$ :

$$\frac{dv_i(t)}{dt} = a \left[ 1 - \left\{ \frac{v_i(t)}{v_0} \right\}^\delta - \left\{ \frac{s^*(v_i(t), \Delta v_{\text{eff}}(t))}{s_{\text{eff}}(t)} \right\}^2 \right], \quad (9)$$

where

$$s^*(v_i(t), \Delta v_{\text{eff}}(t)) = s_0 + \max \left\{ 0, T v_i(t) + \frac{v_i(t) \Delta v_{\text{eff}}(t)}{2 \sqrt{ab}} \right\} \quad (10)$$

is the desired gap of robot  $i$  at time  $t$  [39]. Parameter  $a$  (m/s<sup>2</sup>) is the maximum acceleration,  $b$  (m/s<sup>2</sup>) is the comfortable deceleration,  $s_0$  (m) is the forward spacing in the halting state on the ground,  $v_0$  (m/s) is the desired velocity,  $T$  (s) is the safe time spacing, and  $\delta$  is the exponent. We set these parameters as listed in Table 1.

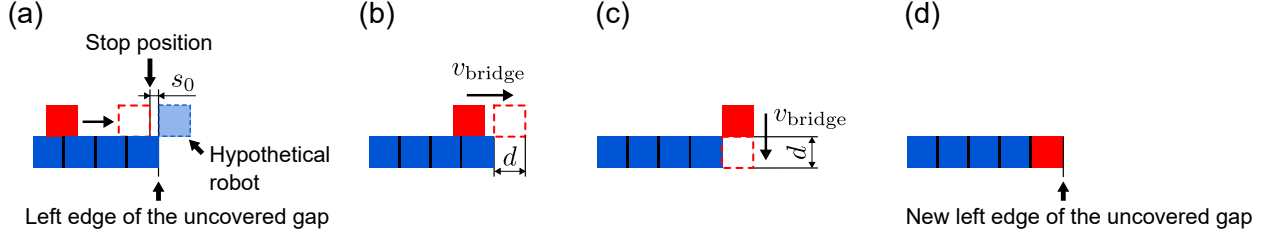


Figure 4: Actions of a robot for self-assembling a bridge. (a) It stops at the position upstream of the left edge of the uncovered gap by  $s_0$  as if a hypothetical robot is stopped at the position downstream of the edge by  $d$ . (b) It moves forward by a distance of  $s_0 + d$  at velocity  $v_{\text{bridge}}$ . (c) It descends by a distance of  $d$  at velocity  $v_{\text{bridge}}$ . (d) It becomes a complete component of the bridge.

If robot  $j$  does not exist and the uncovered gap exists, the target object is the left edge of the uncovered gap. If robot  $j$  exists and the uncovered gap does not exist, the target object is robot  $j$ . If neither robot  $j$  nor the uncovered gap exists, the target object does not exist, and the acceleration of robot  $i$  is given by

$$\frac{dv_i(t)}{dt} = a \left[ 1 - \left\{ \frac{v_i(t)}{v_0} \right\}^\delta \right]. \quad (11)$$

We update  $x_i(t)$  and  $v_i(t)$  at regular time intervals of  $\Delta t = 0.1$  s by

$$x_i(t + \Delta t) = x_i(t) + v_i(t)\Delta t + \frac{a_i(t)(\Delta t)^2}{2} \quad (12)$$

and

$$v_i(t + \Delta t) = v_i(t) + a_i(t)\Delta t, \quad (13)$$

respectively according to the ballistic method [43]. Since the system is periodic, if  $x_i(t + \Delta t) \geq L$ , we subtract  $L$  from  $x_i(t + \Delta t)$ .

### 2.2.2. Self-assembling a bridge

Robot  $i$  stops at the position upstream of the left edge of the uncovered gap by  $s_0$  as if a hypothetical robot is stopped at the position downstream of the edge by  $d$  as shown in Fig. 4(a). Next, robot  $i$  moves forward by a distance of  $s_0 + d$  at velocity  $v_{\text{bridge}}$  (m/s) as shown in Fig. 4(b). Subsequently, robot  $i$  descends by a distance of  $d$  at velocity  $v_{\text{bridge}}$  as shown in Fig. 4(c). In this way, robot  $i$  becomes a complete component of a bridge as shown in Fig. 4(d). Self-assembly of a bridge lasts until the bridge length becomes  $\lambda$  (that is,  $M$  robots become complete components of the bridge). Robots can move forward on the robots that are complete components of a bridge.

It should be noted that the maximum permissible stress [20], and the maximum permissible moment and axial load [25, 26] were considered in self-assembled robot structures. As a first step to investigate the influence of self-disassembly of bridges on the collective flow characteristics of swarm robots, we do not consider the limitations of permissible stress or moment applied to robots. Besides, we simplify the bridge structure as much as possible. That is, the bridge is composed of a single layer of robots similarly to the robot-bridge concept illustrated by Hosokawa et al. [18]. Moreover, the single-layer bridges are maintained till robots start self-disassembling them.

### 2.2.3. Self-disassembling a bridge

Self-disassembling a bridge is prevented in prevent-scenario, and allowed in allow-scenario. Therefore, robots perform the following actions only in allow-scenario. Self-disassembling a bridge is prohibited until self-assembling it is completed (that is, the bridge length becomes  $\lambda$ ). After the bridge length becomes  $\lambda$ , the robot that is the most upstream complete component of the bridge is named *target-robot*. Among the robots that are not complete components of bridges, the robot just downstream of target-robot is named *robot-ahead*, and the robot just upstream

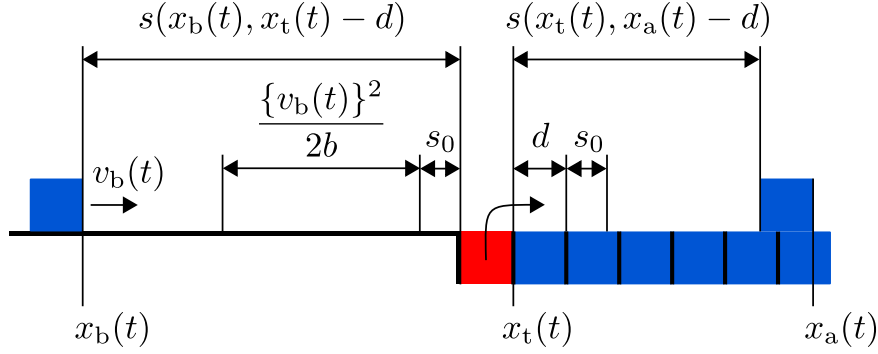


Figure 5: Schematic view of the conditions for target-robot to start self-disassembling a bridge.

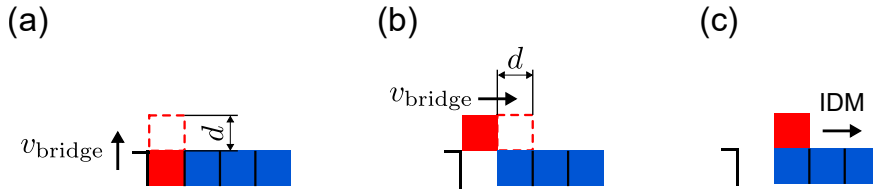


Figure 6: Actions of target-robot for self-disassembling a bridge. (a) It ascends by a distance of  $d$  at velocity  $v_{bridge}$ . (b) It moves forward by a distance of  $d$  at velocity  $v_{bridge}$ , and stops. (c) It resumes following its target object according to IDM.

of target-robot is named *robot-behind*. If only one robot is not a complete component of bridges, this robot is robot-ahead and robot-behind simultaneously. Target-robot checks the following two conditions:

$$s(x_t(t), x_a(t) - d) \geq d + s_0 \quad (14)$$

and

$$s(x_b(t), x_t(t) - d) \geq s_0 + \frac{\{v_b(t)\}^2}{2b}, \quad (15)$$

as illustrated in Fig. 5. Positions  $x_t(t)$  (m),  $x_a(t)$  (m), and  $x_b(t)$  (m) are the positions of target-robot, robot-ahead, and robot-behind at time  $t$ , respectively. Velocity  $v_b(t)$  (m/s) is the horizontal velocity of robot-behind at time  $t$ . Condition (14) prevents target-robot from colliding with robot-ahead. In condition (15),  $\{v_b(t)\}^2 / (2b)$  is the distance required for robot-behind to stop from velocity  $v_b(t)$  at acceleration  $-b$ . Condition (15) denotes that the forward spacing from robot-behind to target-robot  $s(x_b(t), x_t(t) - d)$  should be greater than or equal to the sum of  $s_0$  and this required distance. If an uncovered gap exists in the forward spacing from robot-behind to target-robot, target-robot does not take robot-behind into account in starting its self-disassembling actions by setting  $s(x_b(t), x_t(t) - d)$  in Cond. (15) to a sufficiently large value:  $s(x_b(t), x_t(t) - d) = 10^6$  m. If both the conditions are satisfied, target-robot starts the following self-disassembling actions. First, target-robot ascends by a distance of  $d$  at velocity  $v_{bridge}$  as shown in Fig. 6(a). Second, it moves forward by a distance of  $d$  at velocity  $v_{bridge}$ , and stops as shown in Fig. 6(b). Third, it resumes moving forward from the velocity of zero by following its target object according to IDM as shown in Fig. 6(c). When it starts the third action, it finishes its role as the target robot, and another robot that is the most upstream complete component of the bridge is assigned as the next target-robot. If neither robot-ahead nor robot-behind exists, target-robot starts the self-disassembling actions without checking Conds. (14) or (15). It should be noted that robots are allowed to self-assemble a new bridge while they are self-disassembling a bridge.

### 2.3. Measurement value

To evaluate the transport efficiency of robots, we measure flow  $q$  (robots/s) in a time-space rectangular region with the measurement period  $T_{meas}$  (s) and the system length  $L$  according to Edie's general definition of flow [44]. We

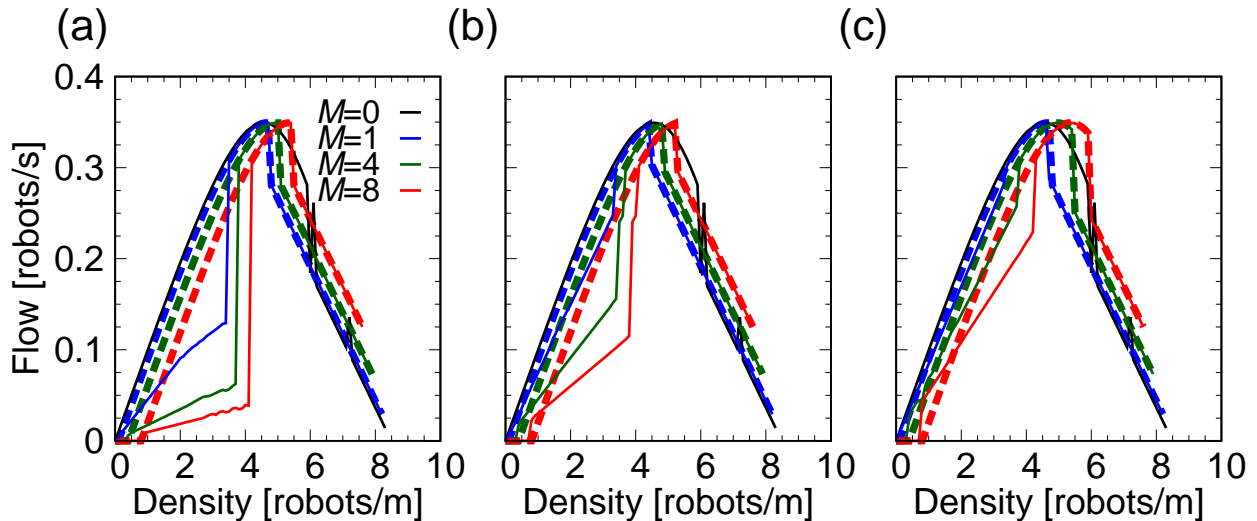


Figure 7: Flow–density diagrams for  $L = 10$  m. (a)  $v_{\text{bridge}} = 0.002$  m/s. (b)  $v_{\text{bridge}} = 0.01$  m/s. (c)  $v_{\text{bridge}} = 0.05$  m/s. The thick dashed blue, dark-green, and red lines denote those for prevent-scenario at  $M = 1, 4$ , and  $8$ , respectively. The thin solid blue, dark-green, and red lines denote those for allow-scenario at  $M = 1, 4$ , and  $8$ , respectively. The thin solid black lines denote those for the scenario with no gap ( $M = 0$ ).

define  $D$  (robots  $\cdot$  m) as the total horizontal distance traveled by all the robots in the system within this region. Flow  $q$  is given by  $D$  divided by the area of this region  $LT_{\text{meas}}$  [44]:

$$q = \frac{D}{LT_{\text{meas}}}. \quad (16)$$

We set  $T_{\text{meas}} = 10^4$  s, which is sufficiently large as a measurement period. To obtain  $q$  at the steady state, we start measuring  $q$  at  $t = 10^5$  s, and finish at  $t = 10^5$  s +  $T_{\text{meas}}$ . We name  $q$  in prevent-scenario and allow-scenario  $q_{\text{prev}}$  and  $q_{\text{allow}}$ , respectively.

### 3. Results

To reveal the relation between flow and density, we have conducted numerical simulations for  $L = 10$  m,  $M = \lambda/d \in \{0, 1, 4, 8\}$ ,  $v_{\text{bridge}} \in \{0.002 \text{ m/s}, 0.01 \text{ m/s}, 0.05 \text{ m/s}\}$ , and  $N \in \{1, 2, \dots, N_{\text{max}}(\lambda)\}$ . Parameter  $N_{\text{max}}(\lambda)$  is the maximum number of robots as a function of  $\lambda$ , and is given by

$$N_{\text{max}}(\lambda) = \left\lfloor \frac{L - \lambda}{s_0 + d} \right\rfloor, \quad (17)$$

where  $\lfloor \cdot \rfloor$  is the floor function such that  $\lfloor x \rfloor = \max \{n \in \mathbb{Z} \mid n \leq x\}$  for  $x \in \mathbb{R}$ . Figures 7(a)–(c) show flow–density ( $q$ – $\rho$ ) diagrams for (a)  $v_{\text{bridge}} = 0.002$  m/s, (b)  $v_{\text{bridge}} = 0.01$  m/s, and (c)  $v_{\text{bridge}} = 0.05$  m/s. We depict the flow–density diagrams for prevent-scenario at  $M = 1, 4$ , and  $8$  with the thick dashed blue, dark-green, and red lines, respectively. We depict those for allow-scenario at  $M = 1, 4$ , and  $8$  with the thin solid blue, dark-green, and red lines, respectively. We depict those for the scenario with no gap ( $M = 0$ ) with the thin solid black lines. Figures 8(a)–(h) show time–space diagrams for allow-scenario. Unless otherwise specified, we set  $N = 10$ ,  $M = 4$ , and  $v_{\text{bridge}} = 0.01$  m/s for these time–space diagrams. Figures 8(a)–(d) show those for  $N = 10, 20, 40$ , and  $60$ , respectively. Figures 8(e) and (f) show those for  $M = 1$  and  $8$ , respectively. Figures 8(g) and (h) show those for  $v_{\text{bridge}} = 0.002$  m/s and  $0.05$  m/s, respectively.

First, we focus on the scenario with no gap. As shown in Figs. 7(a)–(c), flow  $q$  decreases sharply near  $\rho = 6$  robots/m. Below this density, the initial free-flow state is maintained. On the other hand, above this density, the initial free-flow state is not maintained due to the instability of IDM, and the steady state is the jammed state, that



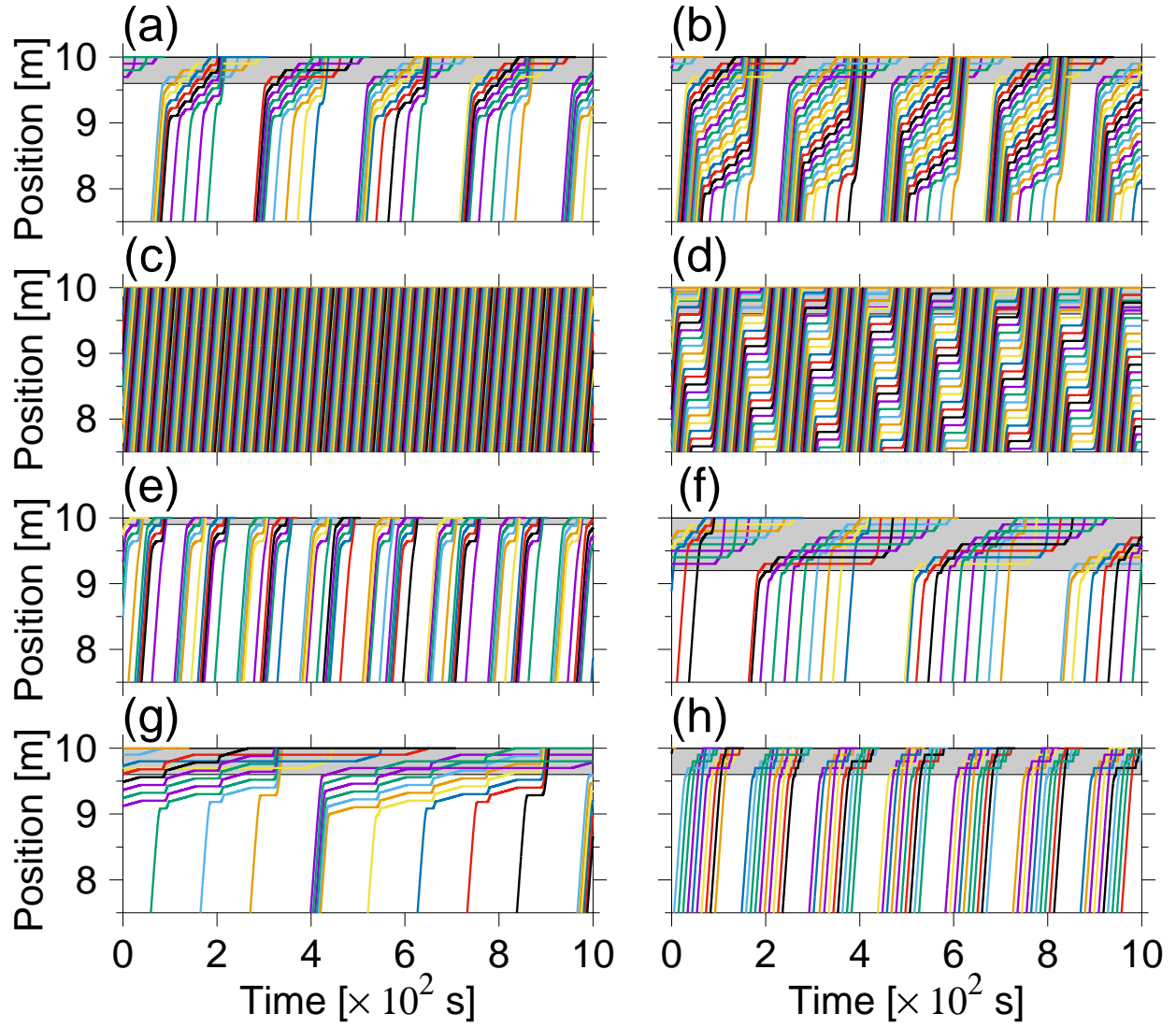


Figure 8: Time–space diagrams for allow-scenario. We set  $L = 10$  m. We shift the display time from the true time by  $-10^5$  s; therefore, the time zero displayed in these diagrams denotes  $t = 10^5$  s. Gray regions denote gaps as guides to the eyes. (a)–(d)  $N = 10, 20, 40,$  and  $60,$  respectively.  $M = 4.$   $v_{\text{bridge}} = 0.01$  m/s. (e) and (f)  $M = 1$  and  $8,$  respectively.  $N = 10.$   $v_{\text{bridge}} = 0.01$  m/s. (g) and (h)  $v_{\text{bridge}} = 0.002$  m/s and  $0.05$  m/s, respectively.  $N = 10.$   $M = 4.$

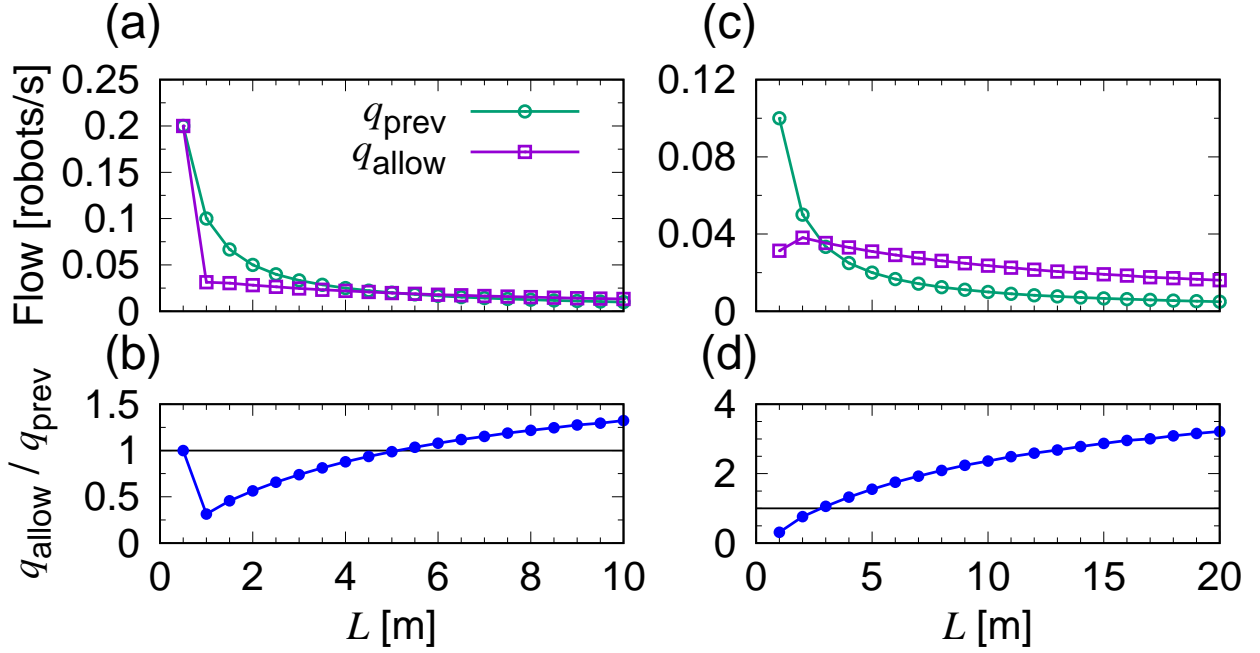


Figure 9: (a) and (c) Flow in prevent-scenario  $q_{\text{prev}}$ , and flow in allow-scenario  $q_{\text{allow}}$  as functions of the system length  $L$ . (b) and (d) Ratio  $q_{\text{allow}}/q_{\text{prev}}$  as a function of  $L$ . The solid black lines denote ratio of 1 as guides to the eyes. We set  $N = 2$  and  $M = 1$  for (a) and (b), and  $N = 5$  and  $M = 4$  for (c) and (d). We set  $v_{\text{bridge}} = 0.01$  m/s. The solid lines through data points are guides to the eyes.

is, the system in the steady state contains a jamming cluster propagating upstream and reducing flow. Such free-flow and jammed steady states are well known in the collective dynamics of SDPs [40–42]. We define  $\rho_{\text{cr, FJ}}$  as the critical density separating the free-flow and jammed steady states. The scenario with no gap exhibits only the two steady states.

Second, we focus on prevent-scenario. As shown in Figs. 7(a)–(c), prevent-scenario also exhibits only the free-flow and jammed steady states. As  $M$  increases, flow–density diagrams shift to the higher-density region. This shift occurs because the increase in  $M$  increases the number of robots becoming bridge components, and decreases the number of robots moving horizontally. Critical density  $\rho_{\text{cr, FJ}}$  increases monotonically as  $M$  increases from 1 to 4 to 8. Critical density  $\rho_{\text{cr, FJ}}$  for prevent-scenario ( $M \geq 1$ ) tends to be smaller than that for the scenario with no gap ( $M = 0$ ) except for the case of  $M = 8$  and  $v_{\text{bridge}} = 0.05$  m/s because self-assembly of bridges disturbs the horizontal movement of robots, and tends to trigger the onset of jamming clusters.

Third, we focus on allow-scenario. In contrast to the scenario with no gap and prevent-scenario, allow-scenario exhibits three steady states in the ascending order of density: the state of repeated self-assembly and self-disassembly of bridges (named the *assembling-disassembling* state) as shown in Figs. 8(a) and (b), the free-flow state as shown in Fig. 8(c), and the jammed state as shown in Fig. 8(d). We define  $\rho_{\text{cr, AF}}$  as the critical density separating the assembling-disassembling and free-flow steady states.

We compare flow–density diagrams for allow-scenario with those for prevent-scenario (Figs. 7(a)–(c)) in the following density regions: (i)  $0 < \rho < \rho_1$ , (ii)  $\rho_1 < \rho < \rho_{\text{cr, AF}}$ , and (iii)  $\rho_{\text{cr, AF}} < \rho \leq N_{\text{max}}(\lambda)/L$ . Density  $\rho_1$  is the threshold density for the order of the magnitude relation between  $q_{\text{prev}}$  and  $q_{\text{allow}}$ , and is much lower than  $\rho_{\text{cr, AF}}$ . (i) When  $\rho$  is extremely low ( $0 < \rho < \rho_1$ ),  $q_{\text{allow}}$  is greater than  $q_{\text{prev}}$  for some parameter settings such as  $M \in \{4, 8\}$  and  $v_{\text{bridge}} \in \{0.01 \text{ m/s}, 0.05 \text{ m/s}\}$ . We investigate  $q_{\text{allow}}$  becoming greater than  $q_{\text{prev}}$  in detail in the later part of this section. (ii) For  $\rho_1 < \rho < \rho_{\text{cr, AF}}$ ,  $q_{\text{allow}}$  is smaller than  $q_{\text{prev}}$  because repeated self-assembly and self-disassembly of bridges disrupt the horizontal movement of robots as shown in Figs. 8(a), (b), (e), and (g). (iii) For  $\rho_{\text{cr, AF}} < \rho \leq N_{\text{max}}(\lambda)/L$ , self-disassembly of bridges no longer occurs in the steady state of allow-scenario as shown in Figs. 8(c) and (d), and  $q_{\text{allow}}$  agrees with  $q_{\text{prev}}$ .

We investigate the influence of  $M$  on  $q_{\text{allow}}$  in the assembling-disassembling state (Figs. 7(a)–(c)). Flow  $q_{\text{allow}}$  in

this state decreases monotonically as  $M$  increases from  $M = 1$  to 4 to 8. This tendency occurs because robots wait for a longer period from joining a bridge to leaving it as  $M$  increases, as shown in the time-space diagrams under  $v_{\text{bridge}} = 0.01$  m/s for  $M = 1, 4,$  and  $8$  (Figs. 8(e), (a), and (f), respectively).

We investigate the influence of  $v_{\text{bridge}}$  on  $q_{\text{allow}}$  in the assembling-disassembling state (Figs. 7(a)–(c)). Flow  $q_{\text{allow}}$  increases monotonically in this state as  $v_{\text{bridge}}$  increases from  $v_{\text{bridge}} = 0.002$  to  $0.01$  to  $0.05$  m/s. The bottleneck effect caused by the repetition of self-assembly and self-disassembly of bridges becomes weaker as  $v_{\text{bridge}}$  increases, as shown in the time-space diagrams under  $M = 4$  for  $v_{\text{bridge}} = 0.002, 0.01,$  and  $0.05$  m/s (Figs. 8(g), (a), and (h), respectively).

Next, we compare  $q_{\text{allow}}$  with  $q_{\text{prev}}$  for various system lengths  $L$  under fixed  $N$  and  $M$ . We set  $v_{\text{bridge}} = 0.01$  m/s. Figures 9(a) and (c) show  $q_{\text{prev}}$  and  $q_{\text{allow}}$  as functions of  $L$  for (a)  $N = 2$  and  $M = 1,$  and (c)  $N = 5$  and  $M = 4.$  Figures 9(b) and (d) show ratio  $q_{\text{allow}}/q_{\text{prev}}$  as a function of  $L$  for the same scenarios as in Figs. 9(a) and (c), respectively.

First, we focus on the case of  $N = 2$  and  $M = 1$  (Figs. 9(a) and (b)). Both  $q_{\text{prev}}$  and  $q_{\text{allow}}$  decrease with respect to  $L$ . Ratio  $q_{\text{allow}}/q_{\text{prev}}$  is 1 at  $L = 0.5$  m because  $L$  is too small to satisfy the conditions to start self-disassembling bridges. Ratio  $q_{\text{allow}}/q_{\text{prev}}$  is smaller than 1 from  $L = 1$  m to nearly 5 m because the repetition of self-assembly and self-disassembly of bridges disrupts the horizontal movement of robots. Ratio  $q_{\text{allow}}/q_{\text{prev}}$  increases with respect to  $L$  for  $L \geq 1$  m. This increase in  $q_{\text{allow}}/q_{\text{prev}}$  occurs for the following two reasons. First, as  $L$  becomes larger under fixed  $N$  and  $M,$  the arrival rate of robots (robots/s) at the gap decreases; therefore, the repetition of self-assembly and self-disassembly of bridges is less likely to disrupt the horizontal movement of robots. Second, self-disassembly of bridges increases the number of robots moving horizontally. Ratio  $q_{\text{allow}}/q_{\text{prev}}$  is greater than 1 for nearly  $L > 5$  m, and reaches 1.32 at  $L = 10$  m. Thus, self-disassembly of bridges can increase the transport efficiency of the system when  $L$  is sufficiently large for fixed  $N$  and  $M.$

Second, we focus on the case of  $N = 5$  and  $M = 4$  (Figs. 9(c) and (d)). Both  $q_{\text{prev}}$  and  $q_{\text{allow}}$  decrease with respect to  $L$  except for  $q_{\text{allow}}$  for  $L < 2$  m. When  $L = 1$  m, which is the minimum value of  $L$  to initially place five robots on the ground (the gap length  $Md = 0.4$  m, and  $N(d + s_0) = 0.6$  m), ratio  $q_{\text{allow}}/q_{\text{prev}}$  is 0.31. Ratio  $q_{\text{allow}}/q_{\text{prev}}$  increases with respect to  $L$  for  $L \geq 1$  m, is greater than 1 for nearly  $L > 3$  m, and reaches 2.36 for  $L = 10$  m, and 3.22 for  $L = 20$  m. Hence ratio  $q_{\text{allow}}/q_{\text{prev}}$  for  $N = 5$  and  $M = 4$  can be greater than that for  $N = 2$  and  $M = 1.$

#### 4. Discussion

We have revealed the following phenomena by numerical simulations. Flow-density diagrams shift to the higher-density region as the gap length becomes larger for both the scenarios preventing self-disassembly of bridges (prevent-scenario) and allowing it (allow-scenario). When density of robots  $\rho$  is low, the steady state of repeated self-assembly and self-disassembly of bridges (the assembling-disassembling state) emerges in allow-scenario. Flow in allow-scenario  $q_{\text{allow}}$  in the assembling-disassembling state is greater than flow in prevent-scenario  $q_{\text{prev}}$  if  $\rho$  is extremely low, or the system length  $L$  is sufficiently large under fixed values of the number of robots  $N$  and the gap-length parameter (the gap length divided by the robot length)  $M.$  Otherwise,  $q_{\text{allow}}$  in this state is smaller than  $q_{\text{prev}}.$  Flow  $q_{\text{allow}}$  in this state increases monotonically with respect to the velocity of robots during joining and leaving bridges  $v_{\text{bridge}}.$  Our results suggest that self-disassembly of bridges in periodic systems is recommended in terms of the transport efficiency of robots only if  $\rho$  is extremely low. Our findings contribute to the development of the collective dynamics of SDPs that self-assemble and self-disassemble structures, and pave the way for elucidating the collective dynamics with other types of self-assembled structures (e.g., ramps [12], chains [13], and towers [13, 45]).

Flow restriction under low-density conditions occurs in not only our system in the assembling-disassembling state, but also the unidirectional, single-lane, and periodic ant traffic system represented by a cellular automaton model [42, 46]. In the ant traffic system, ants attach chemical substance called pheromone to the ground. The probability that an ant moves forward is high or low if the pheromone exists or does not exist just ahead of the cell where the ant is placed, respectively. Flow restriction is caused in the ant traffic system by the evaporation of the pheromone. Both the ant traffic system and our system in allow-scenario have common in that flow restriction is mitigated by a sufficiently large density, whereas the two systems are different with respect to the site-specificity of the bottleneck effect. In the ant traffic system, evaporation of the pheromone occurs irrespective of sites. In our system, self-assembly and self-disassembly of bridges are site-specific, and occur at the gap.

We list some potential future work as follows. Our model has treated single-layer bridges, and has not considered the specifications of robots in detail: (i) the maximum permissible stress, moment or axial force [20, 25, 26], (ii) physical interfaces to attach themselves to other robots [47] or walls, (iii) motion mechanisms for self-assembling the structures [22, 23], (iv) horizontal movement mechanisms, such as tracks or wheels [5, 12, 45], (v) sensors to detect joint positions [48] or terrain changes [6], or (vi) wireless communication devices [49]. We will take these specifications into account for the systems with self-assembled bridges of more complex structures [20, 25, 26] in our future work. We have focused on a unidirectional, single-lane, and periodic system. We will treat other types of systems, such as bidirectional, multi-lane, and/or open systems. Since self-assembly and self-disassembly of bridges cause jamming clusters of robots, removing the clusters is expected to increase the transport efficiency of robots. Removal of the clusters will be achieved by the strategies developed in vehicular traffic flow such as the jam-absorption driving [50, 51]. To introduce the strategies into the swarm robot system warrants our future work.

## References

- [1] E. Şahin, Swarm robotics: From sources of inspiration to domains of application, in: *Swarm Robotics*, Springer, 2005, pp. 10–20. doi:[https://doi.org/10.1007/978-3-540-30552-1\\_2](https://doi.org/10.1007/978-3-540-30552-1_2).
- [2] M. Brambilla, E. Ferrante, M. Birattari, M. Dorigo, Swarm robotics: a review from the swarm engineering perspective, *Swarm Intell.* 7 (1) (2013) 1–41. doi:<https://doi.org/10.1007/s11721-012-0075-2>.
- [3] S. Hirose, T. Shirasu, E. F. Fukushima, Proposal for cooperative robot “Gunryu” composed of autonomous segments, *Robot. Auton. Syst.* 17 (1-2) (1996) 107–118. doi:[https://doi.org/10.1016/0921-8890\(95\)00066-6](https://doi.org/10.1016/0921-8890(95)00066-6).
- [4] H. B. Brown, J. V. Weghe, C. A. Bererton, P. K. Khosla, Millibot trains for enhanced mobility, *IEEE/ASME Trans. Mechatron.* 7 (4) (2002) 452–461. doi:<https://doi.org/10.1109/TMECH.2002.806226>.
- [5] F. Mondada, G. C. Pettinaro, A. Guignard, I. W. Kwee, D. Floreano, J.-L. Deneubourg, S. Nolfi, L. M. Gambardella, M. Dorigo, Swarm-bot: a new distributed robotic concept, *Auton. Robot.* 17 (2) (2004) 193–221. doi:<https://doi.org/10.1023/B:AUR0.0000033972.50769.1c>.
- [6] R. O’ Grady, R. Groß, A. L. Christensen, M. Dorigo, Self-assembly strategies in a group of autonomous mobile robots, *Auton. Robots* 28 (4) (2010) 439–455. doi:<https://doi.org/10.1007/s10514-010-9177-0>.
- [7] C. S. Casarez, R. S. Fearing, Step climbing cooperation primitives for legged robots with a reversible connection, in: *2016 IEEE Int. Conf. Robot. Autom. (ICRA)*, IEEE, 2016, pp. 3791–3798. doi:<https://doi.org/10.1109/ICRA.2016.7487567>.
- [8] H. Asama, M. Sato, N. Goto, H. Kaetsu, A. Matsumoto, I. Endo, Mutual transportation of cooperative mobile robots using forklift mechanisms, in: *1996 IEEE Int. Conf. Robot. Autom. (ICRA)*, IEEE, 1996, pp. 1754–1759. doi:<https://doi.org/10.1109/ROBOT.1996.506966>.
- [9] N. Napp, R. Nagpal, Distributed amorphous ramp construction in unstructured environments, *Robotica* 32 (2014) 279–290. doi:<https://doi.org/10.1017/S0263574714000113>.
- [10] R. Fujisawa, N. Nagaya, S. Okazaki, R. Sato, Y. Ikemoto, S. Dobata, Active modification of the environment by a robot with construction abilities, *ROBOMECH J.* 2 (1) (2015) 1–11. doi:<https://doi.org/10.1186/s40648-015-0030-2>.
- [11] N. Melenbrink, J. Werfel, Local force cues for strength and stability in a distributed robotic construction system, *Swarm Intell.* 12 (2) (2018) 129–153. doi:<https://doi.org/10.1007/s11721-017-0149-2>.
- [12] T. Harada, Y. Sueoka, H. Shigeyoshi, K. Miyoshi, Y. Sugimoto, K. Osuka, Demonstration of cooperative obstacle crossing by sensorless swarm robots based on the mechanical interaction aided field control, *Trans. JSME* 87 (894), article-No. 20–00112 (in Japanese). doi:<https://doi.org/10.1299/transjsme.20-00112>.
- [13] P. Swisler, M. Rubenstein, ReactiveBuild: environment-adaptive self-assembly of amorphous structures, in: *15th Int. Conf. Distrib. Auton. Robot. Syst. (DARS 2021)*, Springer, 2022, pp. 363–375. doi:[https://doi.org/10.1007/978-3-030-92790-5\\_28](https://doi.org/10.1007/978-3-030-92790-5_28).
- [14] B. Hölldobler, E. O. Wilson, The multiple recruitment systems of the african weaver ant *Oecophylla longinoda* (Latreille) (Hymenoptera: Formicidae), *Behav. Ecol. Sociobiol.* 3 (1) (1978) 19–60. doi:<https://doi.org/10.1007/BF00300045>.
- [15] N. R. Franks, Army ants: a collective intelligence, *Am. Scientist* 77 (2) (1989) 138–145.
- [16] B. Hölldobler, E. O. Wilson, *Journey to the ants: a story of scientific exploration*, Belknap Press of Harvard University Press, 1994.
- [17] A. Pamecha, I. Ebert-Uphoff, G. S. Chirikjian, Useful metrics for modular robot motion planning, *IEEE Trans. Robot. Autom.* 13 (1997) 531–545. doi:<https://doi.org/10.1109/70.611311>.
- [18] K. Hosokawa, T. Tsujimori, T. Fujii, H. Kaetsu, H. Asama, Y. Kuroda, I. Endo, Self-organizing collective robots with morphogenesis in a vertical plane, in: *Proc. 1998 IEEE Int. Conf. Robot. Autom. (ICRA)*, IEEE, 1998, pp. 2858–2863. doi:<https://doi.org/10.1109/ROBOT.1998.680616>.
- [19] J. E. Walter, J. L. Welch, N. M. Amato, Concurrent metamorphosis of hexagonal robot chains into simple connected configurations, *IEEE Trans. Robot. Autom.* 18 (6) (2002) 945–956. doi:<https://doi.org/10.1109/TRA.2002.805648>.
- [20] N. Inou, S. Fukushima, N. Shimotai, S. Ujihashi, Study of group robots adaptively forming a mechanical structure: effect of mechanical properties of cellular robots on structure formation, *JSME Int. J. Ser. C* 43 (1) (2000) 127–133. doi:<https://doi.org/10.1299/jsmec.43.127>.
- [21] N. Inou, N. Shimotai, S. Fukushima, H. Ogawa, S. Ujihashi, Study of group robots adaptively forming a mechanical structure: information-processing functions of the cellular robot required for transporting a load to an opposite side, *JSME Int. J. Ser. C* 43 (1) (2000) 134–140. doi:<https://doi.org/10.1299/jsmec.43.134>.
- [22] N. Inou, H. Kobayashi, M. Koseki, Development of pneumatic cellular robots forming a mechanical structure, in: *2002 7th Int. Conf. Control. Autom. Robot. Vision (ICARCV 2002)*, Vol. 1, IEEE, 2002, pp. 63–68. doi:<https://doi.org/10.1109/ICARCV.2002.1234791>.

- [23] N. Inou, K. Minami, M. Koseki, Group robots forming a mechanical structure-development of slide motion mechanism and estimation of energy consumption of the structural formation, in: Proc. 2003 IEEE Int. Symp. Comput. Intell. Robot. Autom., Vol. 2, IEEE, 2003, pp. 874–879. doi:<https://doi.org/10.1109/CIRA.2003.1222295>.
- [24] Y. Suzuki, N. Inou, H. Kimura, M. Koseki, Self-reconfigurable modular robots adaptively transforming a mechanical structure: algorithm for adaptive transformation to load condition, J. Robot. 2011 (2011) Article-ID 794251. doi:<https://doi.org/10.1155/2011/794251>.
- [25] E. Bray, R. Groß, Distributed self-assembly of cantilevers by force-aware robots, in: 2021 Int. Symp. Multi-Robot Multi-Agent Syst. (MRS), IEEE, 2021, pp. 110–118. doi:<https://doi.org/10.1109/MRS50823.2021.9620697>.
- [26] E. Bray, R. Groß, Distributed optimisation and deconstruction of bridges by self-assembling robots, in: Proc. Robot.: Sci. Syst. XVIII, Robotics: Science and Systems Foundation, 2022. doi:<https://doi.org/10.15607/RSS.2022.XVIII.030>.
- [27] J. Nguyen-Duc, M. Mutlu, S. Hauser, A. Barnerdino, A. Ijspeert, Cooperative bridge building by self-reconfigurable modular robots based on ants' stigmergic behaviour, in: 9th Int. Symp. Adapt. Motion Anim. Mach. (AMAM 2019), EPFL, 2019, pp. Paper–No. 71. doi:<https://doi.org/10.5075/epfl-BIOROB-AMAM2019-71>.
- [28] M. Malley, B. Haghighat, L. Houel, R. Nagpal, *Eciton robotica*: design and algorithms for an adaptive self-assembling soft robot collective, in: 2020 IEEE Int. Conf. Robot. Autom. (ICRA), IEEE, 2020, pp. 4565–4571. doi:<https://doi.org/10.1109/ICRA40945.2020.9196565>.
- [29] M. Andrés Arroyo, S. Cannon, J. J. Daymude, D. Randall, A. W. Richa, A stochastic approach to shortcut bridging in programmable matter, Nat. Comput. 17 (4) (2018) 723–741. doi:<https://doi.org/10.1007/s11047-018-9714-x>.
- [30] K. Sugawara, Y. Doi, M. Shishido, Casualty-based cooperation in swarm robots, Artif. Life Robot. 23 (4) (2018) 645–650. doi:<https://doi.org/10.1007/s10015-018-0501-7>.
- [31] J. Paulos, N. Eckenstein, T. Tosun, J. Seo, J. Davey, J. Greco, V. Kumar, M. Yim, Automated self-assembly of large maritime structures by a team of robotic boats, IEEE Trans. Autom. Sci. Eng. 12 (2015) 958–968. doi:<https://doi.org/10.1109/TASE.2015.2416678>.
- [32] D. Saldaña, B. Gabrich, M. Whitzer, A. Prorok, M. F. M. Campos, M. Yim, V. Kumar, A decentralized algorithm for assembling structures with modular robots, in: 2017 IEEE/RSJ Int. Conf. Intell. Robot. Syst. (IROS), IEEE, 2017, pp. 2736–2743. doi:<https://doi.org/10.1109/IROS.2017.8206101>.
- [33] S. Garnier, T. Murphy, M. Lutz, E. Hurme, S. Leblanc, I. D. Couzin, Stability and responsiveness in a self-organized living architecture, PLoS Comput. Biol. 9 (3) (2013) e1002984. doi:<https://doi.org/10.1371/journal.pcbi.1002984>.
- [34] C. R. Reid, M. J. Lutz, S. Powell, A. B. Kao, I. D. Couzin, S. Garnier, Army ants dynamically adjust living bridges in response to a cost–benefit trade-off, Proc. Natl. Acad. Sci. USA 112 (49) (2015) 15113–15118. doi:<https://doi.org/10.1073/pnas.1512241112>.
- [35] M. J. Lutz, S. Powell, I. D. Couzin, An agent-based model to simulate the formation and dynamics of self-assembled structures in army ants, in: IEEE 3rd Int. Workshops Found. Appl. Self\* Syst. (FAS\*W), IEEE, 2018, pp. 142–146. doi:<https://doi.org/10.1109/FAS-W.2018.00039>.
- [36] H. Ishiwata, N. Noman, H. Iba, Emergence of cooperation in a bio-inspired multi-agent system, in: AI 2010: Adv. Artific. Intell., Springer, 2011, pp. 364–374. doi:[https://doi.org/10.1007/978-3-642-17432-2\\_37](https://doi.org/10.1007/978-3-642-17432-2_37).
- [37] T. Ichimura, Y. Douzono, Altruism simulation based on pheromone evaporation and its diffusion in army ant inspired social evolutionary system, in: 6th Int. Conf. Soft Comput. Intell. Syst., 13th Int. Symp. Adv. Intell. Syst., IEEE, 2012, pp. 1357–1362. doi:<https://doi.org/10.1109/SCIS-ISIS.2012.6505135>.
- [38] M. Treiber, A. Hennecke, D. Helbing, Congested traffic states in empirical observations and microscopic simulations, Phys. Rev. E 62 (2) (2000) 1805–1824. doi:<https://doi.org/10.1103/PhysRevE.62.1805>.
- [39] M. Treiber, A. Kesting, Traffic flow dynamics: data, models and simulation, Springer, 2013.
- [40] D. Chowdhury, L. Santen, A. Schadschneider, Statistical physics of vehicular traffic and some related systems, Phys. Rep. 329 (4-6) (2000) 199–329. doi:[https://doi.org/10.1016/S0370-1573\(99\)00117-9](https://doi.org/10.1016/S0370-1573(99)00117-9).
- [41] D. Helbing, Traffic and related self-driven many-particle systems, Rev. Mod. Phys. 73 (4) (2001) 1067–1141. doi:<https://doi.org/10.1103/RevModPhys.73.1067>.
- [42] A. Schadschneider, D. Chowdhury, K. Nishinari, Stochastic transport in complex systems: from molecules to vehicles, Elsevier, 2010.
- [43] M. Treiber, V. Kanagaraj, Comparing numerical integration schemes for time-continuous car-following models, Physica A 419 (2015) 183–195. doi:<https://doi.org/10.1016/j.physa.2014.09.061>.
- [44] L. C. Edie, Discussion of traffic stream measurements and definitions, in: Proc. 2nd Int. Symp. Theory Traffic Flow, OECD, 1965, pp. 139–154.
- [45] L. Cucu, M. Rubenstein, R. Nagpal, Towards self-assembled structures with mobile climbing robots, in: 2015 IEEE Int. Conf. Robot. Autom. (ICRA), IEEE, 2015, pp. 1955–1961. doi:<https://doi.org/10.1109/ICRA.2015.7139454>.
- [46] D. Chowdhury, V. Guttal, K. Nishinari, A. Schadschneider, A cellular-automata model of flow in ant trails: non-monotonic variation of speed with density, J. Phys. A 35 (41) (2002) L573–L577. doi:<https://doi.org/10.1088/0305-4470/35/41/L03>.
- [47] P. Swisler, M. Rubenstein, FireAnt3D: a 3D self-climbing robot towards non-latticed robotic self-assembly, in: 2020 IEEE/RSJ Int. Conf. Intell. Robots Syst. (IROS), IEEE, 2020, pp. 3340–3347. doi:<https://doi.org/10.1109/IROS45743.2020.9341116>.
- [48] E. H. Østergaard, K. Kassow, R. Beck, H. H. Lund, Design of the ATRON lattice-based self-reconfigurable robot, Auton. Robots 21 (2) (2006) 165–183. doi:<https://doi.org/10.1007/s10514-006-8546-1>.
- [49] S. Tang, Y. Zhu, J. Zhao, X. Cui, The UBot modules for self-reconfigurable robot, in: Proc. 2009 ASME/IFTOMM Int. Conf. Reconfigurable Mech. Robot. (ReMAR 2009), IEEE, 2009, pp. 529–535.
- [50] R. Nishi, A. Tomoeda, K. Shimura, K. Nishinari, Theory of jam-absorption driving, Transp. Res. B 50 (2013) 116–129. doi:<https://doi.org/10.1016/j.trb.2013.02.003>.
- [51] Y. Taniguchi, R. Nishi, T. Ezaki, K. Nishinari, Jam-absorption driving with a car-following model, Physica A 433 (2015) 304–315. doi:<https://doi.org/10.1016/j.physa.2015.03.036>.